Efficient Removal of Cr (VI) from Aqueous Solution with PPy-Fe_3O_4 Nanocomposite

A.M. Muliwa and M.S. Onyango

***Abstract*—** Polypyrrole-magnetite (PPy-Fe_3O_4) nanocomposite (NC) was synthesized, characterized and tested for its ability to remove hexavalent Cr (VI) from aqueous solution. X-ray diffraction (XRD) analysis showed crystalline structure in the NC while magnetic measurements revealed super-paramagnetic properties. Batch adsorption kinetic studies indicated a strong influence of quantity of Fe_3O_4 and initial Cr (VI) concentration to the sorption capacity. Kinetic data fitted well to pseudo-second order kinetic model suggesting a chemisorption process. Finally, both intra-particle and film diffusion mechanisms controlled the adsorption process.

***Keywords*—**Adsorption, hexavalent chromium, polypyrrole-magnetite

I. Introduction

The increasing contamination of industrial and urban wastewater by toxic heavy metals is a worrying environmental and public health problem. One of the toxic heavy metals is chromium which is found in industrial effluents from electroplating facilities, electrolytic refining plants, acid mine plants, tanneries and textile plants among others [1][2]. Chromium primarily exists in trivalent Cr (III) and hexavalent forms Cr (VI) in the aquatic environment. The public is more concerned about Cr (VI) because its toxicity is 100 times higher than Cr (III), and it can seriously damage people's health due to its teratogenicity, mutagenicity, and carcinogenicity in biological systems. The proposed limit of Cr (VI) in surface discharge and drinking water by the US EPA is 0.10 mg/L and 0.05 mg/L, respectively [3]. Therefore, Cr (VI) must be removed and recovered from polluted waste streams so as to comply with the tight environmental quality regulations [4].

The most commonly used methods for removal of Cr (VI) from aqueous solutions include precipitation, ion-exchange, reverse osmosis and electrocoagulation and adsorption [5]. Among these technologies, adsorption stands out as a technically feasible, simple, socially acceptable, fast, and economically viable method which does not generate secondary waste [6]. However, the success of an adsorption process depends very strongly on the quality of adsorbent. This has led to design and development of nanostructured adsorbents which offer large surface area to volume ratio, fast kinetics and high adsorption capacity [7]. A major problem with nanostructured sorbents is their separation from aqueous environment because their small size limits their applications in filtration and fixed bed mechanisms where high pressure drops are often developed.

Recently, magnetic nanoadsorbents have emerged strongly as candidates materials that could provide permanent solutions to solid-liquid separation processes. This is because after adsorption, they can be retrieved from aqueous media by external magnetic field. The commonly used magnetic nanoparticles are magnetite (Fe_3O_4) because of their simplicity in preparation and they possess super-paramagnetic properties. However, naked Fe_3O_4 NPs are prone to air oxidation and easily aggregate in solution hence their stabilization by surface modification is important [8]. Therefore, use of polypyrrole (PPy) to encapsulate Fe_3O_4 NPs would overcome these challenges materials because PPy and its derivatives has been widely used for extraction of various types of compounds. The encapsulation of Fe_3O_4 NPs creates an adsorbent with improved dispersion properties, and one that can be separated magnetically thus it can be applied selectively in adsorbing certain kinds of compounds from different matrices.

In this study, we synthesized and characterized three grades of PPy-Fe_3O_4 NCs as a scavengers for mobile and toxic Cr (VI) using our previously reported method [9]. The sorption capacities of the NCs were explored through batch adsorption kinetic experiments for different initial Cr (VI) concentration. Thereafter, sorption kinetic data was fitted to existing kinetic models to extract important parameters that would aid in designing an adsorption system.

II. Materials and Methods

2.1 Materials: Pyrrole (Py) monomer (98%), anhydrous ferric chloride ($FeCl_3$) and potassium dichromate ($K_2Cr_2O_7$) were purchased from Merck (Pty) Ltd (South Africa) while 1, 5-diphenylcarbazide were supplied by Sigma-Aldrich (Germany). All other chemicals were of analytical reagent (AR) grade and were used as received.

2.2 Preparation of the adsorption media: Magnetite (Fe_3O_4) nanoparticles were prepared through standard co-precipitation method [8] while PPy-Fe_3O_4 NCs with 40.3%, 50.4% and 58.5% Fe_3O_4 loadings were synthesized using our previous method [9].

2.3 Characterization: The crystalline structure for the three grades of PPy-Fe_3O_4 nanocomposite was analyzed using X-ray diffraction (XRD) scans performed on specimens using Panalytical X'pert PRO diffractometer 3060/60 with Cu Kα (λ=0.154 nm) monochromated radiation source with variable slits operated at 45 kV/40 mA. Magnetic measurements were

A.M. Muliwa & M.S. Onyango, Department of Chemical, Metallurgical and Materials Engineering, Tshwane University of Technology (corresponding author phone: +27123823533; fax: +27123823533; e-mail: OnyangoMS@tut.ac.za).

done at room temperature (300 K) with superconducting quantum interference devices (SQUIDs with applied field in the range of -2T to 2T.

2.4 Sorption dynamic studies. Adsorption kinetics experiments were conducted in the continuously stirred tank reactor (CSTR) under varied conditions. In short, 4 g of each of 40.3 %, 50.4 % and 58.5% NCs were dispersed in 5 litres containing 100 mg/L Cr (VI) aqueous solution at room temperature. The solutions pH was adjusted to 2 (optimised elsewhere [9]) using 0.1 M HCl or 0.1 M NaOH while stirring the solution at 300 rpm. Samples (5 mL) were collected at predetermined time intervals for a period of 6 hours. Analysis of residual Cr (VI) ions in the collected samples was done with UV-Vis spectrophotometer (1800-Shimadzu, Japan) at wavelength of 542 nm using the standard diphenylcarbazide method [10]. Finally, Cr (VI) removal percentage was computed according to (1) below.

$$\frac{C_o - C_t}{C_o} \times 100 \qquad (1)$$

where C_o and C_t are initial and time, *t*, concentrations (mg/L) of Cr (VI) ions, respectively. Experiments were repeated using 50 and 150 mg/L of Cr (VI) ions.

III. RESULTS AND DISCUSION

3.1 Characterization

3.1.1*X-ray Diffraction Analysis.* Fig. 2 shows the XRD measurements obtained for 40.3 %, 50.4 % (before and after adsorption) and 58.5 % PPy-Fe_3O_4 NCs. Six characteristic peaks are observed at 2 theta 30.13, 35.49, 43.13, 53.55, 62.63, and 57.03, which is attributed to (220), (311), (400), (422), (440), and (511) planes of Fe_3O_4. The low intensities and background noise observed are caused by the amorphous polypyrrole shell [11].These observations demonstrate that all the as-prepared PPy-Fe_3O_4 nanocomposites display crystalline magnetite structure [12].

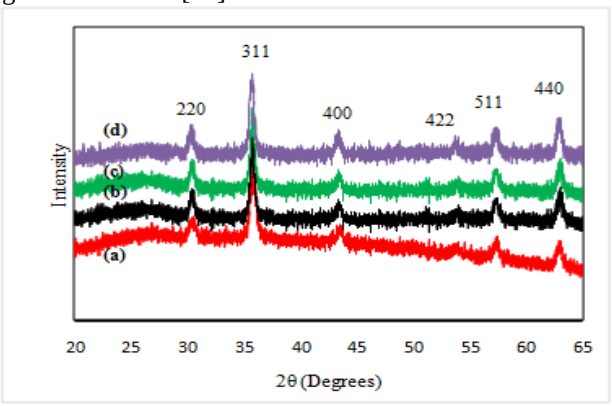

Fig. 1 X-ray diffraction (XRD) characterization of PPy-Fe_3O_4 nanocomposites (a) 40.3%, (b) and (c) is 50.4% (before and after adsorption) and (d) 58.5%

3.1.2*Magnetic Measurements.* Figure 4 shows magnetization, M vs applied field, T plot obtained for 50.4% PPy-Fe_3O_4 NC as an example. The magnetizations saturation (M_s) obtained is 30.20 emu/g which is low compared to that of bulk Fe_3O_4 nanoparticles (M_s= 84 emu/g). The absence of hysteresis loops, remanance magnetism and coercivity as observed confirms that the NCs is super-paramagnetic [13]. Therefore, the NCs meets the minimum criterion for successful magnetic separation of a material from a solution by use of conventional methods which requires a material to possess a M_s value higher than 16 emu/g [14].

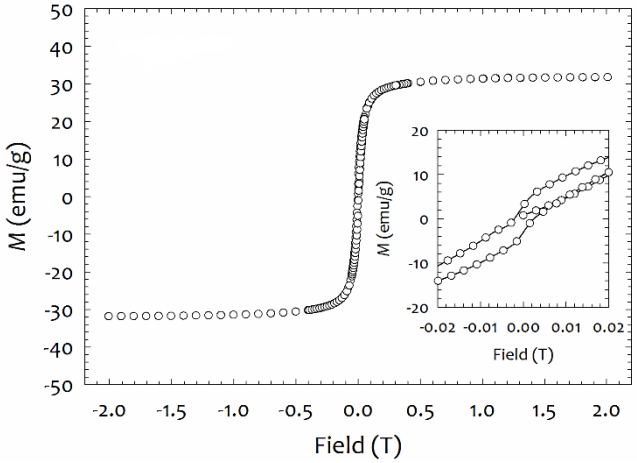

Fig. 2 Magnetic measurements for 50.4% Fe_3O_4 loaded PPy-Fe_3O_4 NC.

3.2 Adsorption dynamic studies

3.2.1*Effect of Fe_3O_4 NPs loadings to Cr (VI) removal.* Fig. 5 shows time dependent % Cr (VI) removal for 40.3 %, 50.4 % and 58.5% PPy-Fe_3O_4 NCs. It is seen that 95% Cr (VI) removal which corresponds to an uptake of 119 mg/g was achieved with 50.4% NC, while 58.5% and 40.3% NCs scavenged 87% (109 mg/g) and 82% (103 mg/g), respectively. Moreover, a rapid adsorption process is observed initially which later reduces between 150-180 minutes as the system approaches equilibrium. Yen et al.[15] observed that increasing Fe_3O_4 NPs in the PPy matrices alters the NCs structure from spherical to tube-like. Therefore, this could be the reason as to why 58.5% NC gave low capacity Cr (VI).

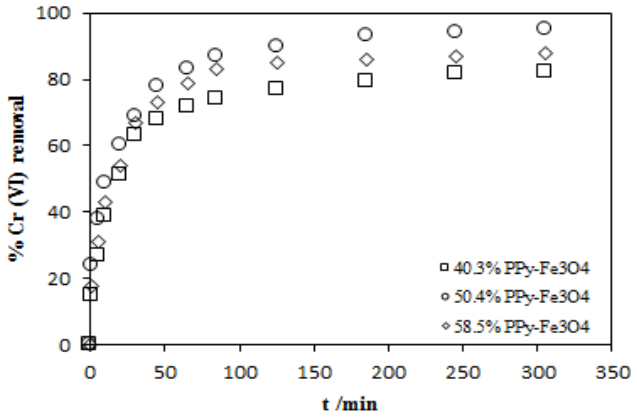

Fig. 3 Time depended % Cr (VI) removal for 40.3% 50.4%, and 58.5% PPy-Fe_3O_4 NCs (100 mg/l of Cr (VI); Temp: 22ºC; 300 rpm; Volume: 5 L and pH 2)

3.2.2*Sorption concentration dependence.* The effect of initial concentration of Cr (VI) ions on adsorption efficiency using 50.4% NC is illustrated in Fig. 7. The sorption rate is seen to increase with increase in initial Cr (VI) concentration and for 50 mg/l, the saturation is reached after 30 minutes, while approximately 150 min was required for 100 and 150 mg/l. The sorption uptake increases from 63 to 144 mg/g as the

initial Cr (VI) concentration is increased from 50 to 150 mg/l, respectively. This phenomenon is attributed to the increase in rate of accumulation of Cr (VI) ions on PPy-Fe_3O_4 NCs which is a function concentration gradient (driving force) according to linear driving force law [3][9][16]. Also, the improved ratio of total active sites to the total Cr (VI) ions in solution which leads to full interactions of Cr (VI) ions with the active sites contributes to these observations. Thus the sorption capacities are significantly influenced by the initial Cr (VI) concentrations.

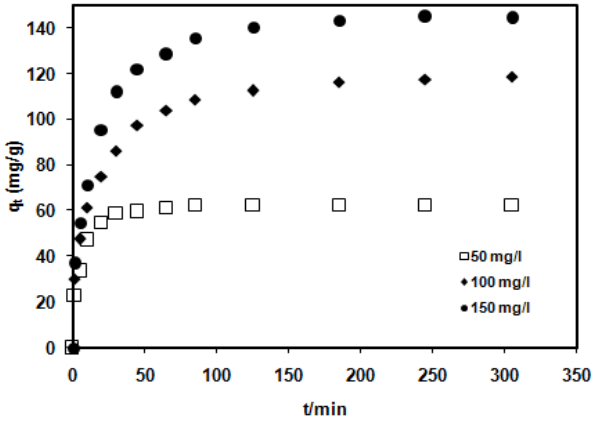

Fig. 4 Time dependent Cr (VI) uptake on 50.4% PPy-Fe_3O_4 NCs for different initial concentrations (pH=2, 300 rpm, Volume = 5 liters)

Kinetic data was evaluated using linear pseudo first-order kinetic model, pseudo second-order, and Elovich models as per (2), (3) and (4).

$$log(q_e - q_t) = log q_e - \frac{k_1}{2.303} \quad (2)$$

$$\frac{t}{q_t} = \frac{1}{k_2 q_e^2} + \frac{t}{q_e} \quad (3)$$

$$q_t = \frac{1}{\beta}\ln(\alpha\beta) + \frac{1}{\beta}\ln t \quad (4)$$

where q_t and q_e represents the amount of Cr (VI) (mg/g) sorbed at time *t* and at equilibrium, respectively, and k_1 is the pseudo first-order rate constant (min^{-1}). Linear relationships were obtained by plotting $log(q_e - q_t)$ against t from where the values of q_e and k_1 were determined from the slope and intercept, respectively. Pseudo first-order assumes that the rate limiting step is physisorption which involves Van der Waal forces, hydrogen bonding and π-π interactions between the sorbate and the sorbent [17] k_2 is the rate constant for pseudo second-order adsorption (g/mg/min). If the adsorption follows a second model then a plot of t/q_t versus *t* should yield a linear relationship and parameters can be extracted accordingly. Pseudo second-order assumes a chemisorption process which involves exchange or sharing of electrons between the sorbent and the sorbate takes place [18]. α and β is the initial adsorption rate (mg/g.min) and desorption constant (g/mg.min) for any one given experiment, respectively. Parameters were calculated from the plot of q_t versus $\ln t$ accordingly. Elovich equation is used to describe chemisorption kinetics and it assumes that the sorbent surface is heterogeneous in nature [19][20].

Fig. 6 shows plots for pseudo-second order linear kinetic model predictions of the Cr (VI) sorption on 50.4% NC as an example. The correlation coefficient values, R^2, obtained are close to unity (above 0.9900) and the rate constants (k_2) decreased from 0.0071 to 0.0009 mg/g/min with increase in concentration. Furthermore, the calculated equilibrium sorption uptake, q_{ecal} which were 63, 119 and 144 mg/g, for linear pseudo second model closer to the experimental equilibrium uptake, q_{emeas} (63,122,147 mg/g) contrary to linear pseudo first-order and Elovich models (see parameters in Table 1). These findings confirms that sorption of Cr (VI) on PPy-Fe_3O_4 NC is well described using linear pseudo second order model which assumes that the rate limiting step may be chemical adsorption involving valence forces through sharing or exchange of electrons between adsorbent surface and Cr (VI) [20].

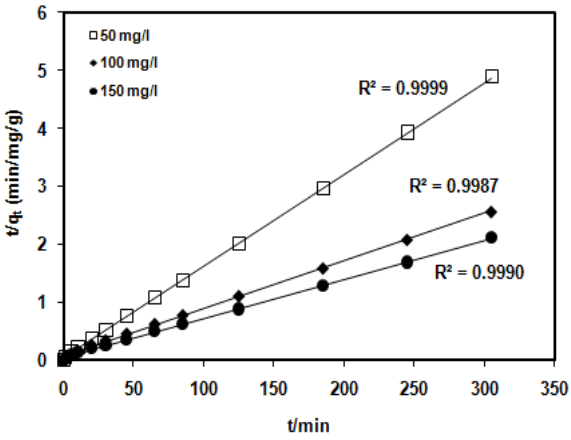

Fig. 5 Linearised fits for pseudo second order kinetic model (100 mg/l of Cr (VI), 4 g of 50.4% PPy-Fe_3O_4 nanocomposite, 22°C, 300 rpm, 5 liters and pH 2)

The adsorption rate controlling step was investigated by intra-particle diffusion model by Weber and Morris (5) and film diffusion model (Boyd model) (6) [21] [22].

$$q_t = k_{id} t^{0.5} + C \quad (5)$$

where q_t is the amount of adsorption in mg/g at any time$t$, k_{id} is the intra-particle diffusion rate constant ($mg/g/min^{0.5}$) and C (mg/g) is a constant that represents the boundary layer thickness.

$$-ln\left(1 - \frac{q_t}{q_e}\right) = k_p t \quad (6)$$

where k_p is the adsorption rate constant. The intra-particle exhibited a multi-linearity characteristic with two steps being involved in the whole adsorption process [23]. The first step represents external surface or instantaneous adsorption process followed by the equilibrium step. Film diffusion model (plots not shown) reveals the plots did not pass through the origin and that lower correlation coefficients were obtained. These findings confirms that the adsorption process is governed by both intra-particle diffusion and external surface sorption. A summary of calculated parameters is given in Table 1 below.

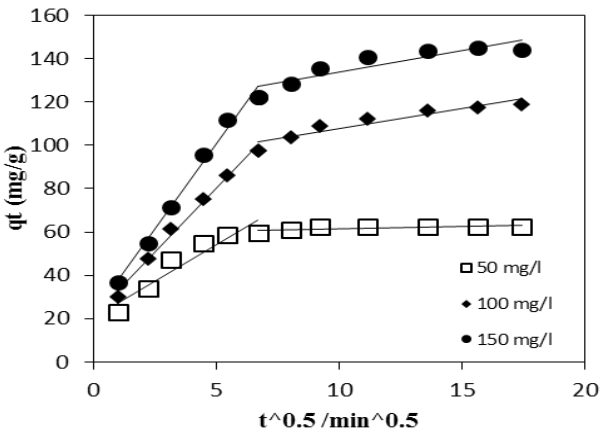

Fig. 6. The intra-particle diffusion model plot

Table 1. Kinetic parameters for Cr (VI) sorption onto 50.4% PPy-Fe_3O_4 nanocomposite.

Model	Parameters	Conc. (mg/L) 50	100	150
Pseudo-first-order	q_e (mg/g)	40.37	88.36	116.04
	k_1 (min^{-1})	0.0682	0.0297	0.0396
	R^2	0.9282	0.953	0.9691
Pseudo-second-order	q_e (mg/g)	63.29	122	147.05
	k_2 (g/mg.min)	0.0071	0.001	0.0009
	R^2	0.9999	0.9987	0.999
Elovich	α (mg/g.min)	363.72	79.49	94.08
	β (g/mg)	0.1402	0.058	0.0464
	R^2	0.9572	0.9751	0.8705
Intra-particle (Weber Morris)	K_{id1} ($mg/g.min^{0.5}$)	6.6945	11.7978	15.7006
	R^2	0.9048	0.9919	0.9899
	K_{id2} ($mg/g.min^{0.5}$)	0.3405	1.8437	1.9676
	R^2	0.5676	0.8881	0.8172
Film diffusion model	k_F	0.0522	0.0171	0.0258
	R^2	0.9723	0.9671	0.9902

IV. Conclusions

The as-synthesized PPy-Fe_3O_4 NCs were found to be super-paramagnetic with crystalline structure and good adsorption capacities for Cr (VI). Sorption kinetic studies demonstrated that Cr (VI) removal highly depends on Fe_3O_4 NPs loadings in the NCs. Chemisorption mechanisms well described the adsorption process with kinetic data fitting well to pseudo-second-order kinetic model. Consequently, adsorption is governed by both intra-particle and film diffusion. These findings demonstrated that the sorbent can be used to scavenge Cr (VI) and thereafter can be separated magnetically with external magnetic field

V. Acknowledgements

The authors would like to acknowledge The National Research Foundation (NRF), South Africa for supporting this Project.

References

[1] K. R. A. Sidhaarth, J. Jeyanthi, and N. Suryanarayanan, "Comparative Studies of Removal of Lead and Zinc from Industrial Wastewater and Aqueous Solution by Iron Oxide Nanoparticle: Performance and Mechanisms," *European Journal of Scientific Research*, vol. 70, no. 2, pp. 169-184, 2012.

[2] Y. Zhao, S. Yang, D. Ding *et al.*, "Effective adsorption of Cr (VI) from aqueous solution using natural Akadama clay," *Journal of Colloid and Interface Science*, vol. 395, pp. 198–204, 2013.

[3] E. Malkoc, Y. Nuhoglu, and M. Dundar, "Adsorption of chromium (VI) on pomace-An olive oil industry waste: Batch and column studies," *Journal of Hazardous Materials*, vol. B138, pp. 142–151, 2006.

[4] Q. Wang, Y. Guan, X. Ren *et al.*, "Application of magnetic extractant for the removal of hexavalent chromium from aqueous solution in high gradient magnetic separator," *Chemical Engineering Journal*, vol. 183, pp. 339– 348, 2012.

[5] J. Hu, Lo, M. C. Irene *et al.*, "Comparative study of various magnetic nanoparticles for Cr (VI) removal," *Separation and Purification Technology*, vol. 56, pp. 249-256, 2007.

[6] H. Li, Z. Li, T. Ting Liu *et al.*, "A novel technology for biosorption and recovery hexavalent chromium in wastewater by bio-functional magnetic beads," *Bioresource Technology*, vol. 99, pp. 6271–6279, 2008.

[7] S. Laurent, D. Forge, M. Port *et al.*, "Magnetic iron oxide nanoparticles: Synthesis, stabilization, vectorization, physicochemical characterizations and biological applications," *Chemical Reviews*, vol. 108, pp. 2064-2110, 2008.

[8] D. Maity, and D. C. Agrawal, "Synthesis of Iron Oxide Nanoparticles under Oxidizing Environment and Their Stabilization in Aqueous and Non-Aqueous Media," *Journal of Magnetism and Magnetic Materials*, vol. 308, pp. 46–55, 2007.

[9] M. Bhaumik, K. Setshedi, A. Maity *et al.*, "Chromium(VI) removal from water using fixed bed column of polypyrrole/Fe_3O_4 nanocomposite," *Separation and Purification Technology*, vol. 110, pp. 11–19, 2013.

[10] APHA, AWWA, and WEF, *Standard Methods for the Examination of Water and Wastewater*, 19 ed., Washington, USA: APHA, 1998.

[11] A. Nan, R. Turcu, I. Bratu *et al.*, "Novel magnetic core-shell Fe_3O_4 polypyrrole nanopaticles functionalized by peptides or albumin," *ARKIVOC*, vol. X, pp. 185-195, 2010.

[12] M. Bhaumik, A. Maity, V. V. Srinivasu *et al.*, "Enhanced removal of Cr (VI) from aqueous solution using Polypyrrole/Fe_3O_4 magnetic nanocomposite," *Journal of Hazardous Materials*, vol. 190, pp. 381-390, 2011.

[13] W. Chen, X. Li, G. Xue *et al.*, "Magnetic and conducting particles: preparation of Polypyrrole layer on Fe_3O_4 nanospheres," *Applied Surface Science*, vol. 218, pp. 215–221, 2003.

[14] X. Zhang, S. Xie, M. C. Paau *et al.*, "Ultrahigh performance liquid chromatographic analysis and magnetic preconcentration of polycyclic aromatic hydrocarbons by Fe_3O_4-doped polymeric nanoparticles," *Journal of Chromatography A*, vol. 1247, pp. 1– 9, 2012.

[15] S. J. Yen, E. C. Chen, R. K. Chiang *et al.*, "Preparation and characterization of polypyrrole/magnetite nanocomposites synthesized by in situ chemical oxidative polymerization," *Journal of Polymer Science B; Polymer Physics*, vol. 46, pp. 1291–1300, 2008.

[16] F. W. Meng, "Study on a Mathematical Model in Predicting Breakthrough Curves of Fixed-bed Adsorption onto Resin Adsorbent," Nanjing, 2005.

[17] H. Li, G. Huang, C. An *et al.*, "Removal of Tannin from Aqueous Solution by Adsorption onto Treated Coal Fly Ash: Kinetic, Equilibrium, and Thermodynamic Studies," *Industrial and Engineering Chemistry Research*, vol. 52, pp. 15923-15931, 2013.

[18] D. Mohan, K. P. Singh, and V. K. Singh, "Trivalent chromium removal from wastewater using low cost activated carbon derived from agricultural waste material and activated carbon fabric cloth," *Journal of Hazardous Materials*, vol. 135, no. 1−3, pp. 280−295, 2006.

[19] K. Johari, N. Saman, S. T. Song *et al.*, "Utilization of Coconut Milk Processing Waste as a Low-Cost Mercury Sorbent," *Industrial & Engineering Chemistry Research*, vol. 52, pp. 16648-15657, 2013.

[20] S. Li, X. Liu, W. Huang *et al.*, "Magnetically assisted removal and separation of cationic dyes from aqueous solution by magnetic nanocomposite hydrogels," *Polymers for Advanced Technologies*, vol. 22, pp. 2439–2447, 2010.

[21] W. J. Weber, and J. C. Morris, "Advances in water pollution research: removal of biologically resistant pollutant fromwastewater by adsorption." pp. 231–266.

[22] W. J. Weber, and J. C. Morris, "Kinetics of adsorption on carbon from solution," *Journal of the Sanitary Engineering Division:American Society of Civil Engineering*, vol. 89, pp. 31-60, 1963.

[23] F. C. Wu, R. L. Tseng, and R. S. Juang, "Initial behaviour of intraparticle diffusion model used in the description of adsorption kinetics," *Chemical Engineering Journal*, vol. 153, pp. 1–8, 2009.